Thickness imaging of evaporating liquid water films by simultaneous Tracer LIF, Raman imaging and Diode Laser Absorption Spectroscopy

D. Greszik, H. Yang, T. Dreier[1*], C. Schulz
Institut für Verbrennung und Gasdynamik (IVG), and Center for Nanointegration (CENIDE)
University of Duisburg-Essen, Germany

Abstract

Knowledge about the thickness of liquid films is important, e.g., in flash boiling of fuel spray impingement on cylinder walls in internal combustion engines or of aqueous urea solutions and subsequent evaporation on exhaust pipes of Diesel engines during exhaust gas after-treatment in the selective catalytic reduction (SCR) of nitrogen oxides. For purposes of process optimization and for providing validation data in CFD-based modeling of these processes, non-intrusive, quantitative liquid film thickness measurement techniques are desired, which potentially provide two-dimensional imaging capabilities and/or high data rates for temporally resolved measurements of the liquid film thickness is required. In this work we present the application of two imaging-based laser-diagnostic techniques – laser-induced fluorescence (LIF) and spontaneous Raman scattering (RS) – as well as a point measurement method – near-infrared diode laser absorption spectroscopy (NIR-DLAS) – for the simultaneous measurement of liquid film thickness during the time-varying evolution of spray-deposited liquid water droplets on transparent surfaces, with specific applications in an air-fed flow duct.

Introduction

Knowledge about the thickness of liquid films is important in many practical processes, such as flash boiling of fuel films in internal combustion engines [1], or the impingement of sprays of aqueous urea solutions and subsequent evaporation in the exhaust pipes of Diesel engines during exhaust gas after-treatment for the selective catalytic reduction (SCR) of nitrogen oxides [2]. For purposes of process optimization and for providing validation data for CFD-based modeling of these processes, non-intrusive, quantitative and often spatially extended measurement techniques for liquid film thickness is desired. In this work we present the application of two imaging-based laser-diagnostic techniques – laser-induced fluorescence (LIF) and spontaneous Raman scattering (RS) – as well as a point measurement method – near-infrared diode laser absorption spectroscopy (NIR-DLAS) – for the measurement of liquid water film thickness (LIF, Raman), as well as liquid film temperature and vapor phase temperature above the film (NIR-DLAS) of water, recently developed in our lab. The latter method already permits data recording rates of several kHz for the simultaneous measurement of these parameters with reasonable temporal resolution during, e.g., spray deposition of liquid water films on the wall of an air-fed flow duct.

Theoretical background

Since liquid water is a non-fluorescent substance when excited with near-ultraviolet radiation, in laser-induced fluorescence (LIF) a molecular species needs to be added in small concentrations, which ideally should fulfill the desirable properties as a fluorescence tracer of good solubility, high fluorescence quantum yield in the UV/VIS spectral region and a co-evaporative behavior with the solvent. In this respect various small ketone-like or aromatic tracer species have been used in the past as tracers in non-fluorescent gases and liquid fuels for imaging mixing processes or temperature. This generally is accomplished by tracer excitation with spatially expanded laser beams of fixed frequency and detection with intensified CCD cameras. A review on tracer LIF fundamentals and applications for gas-phase measurements is given in [3]. For a tracer species of concentration n_{tr} dissolved in liquid water which forms a film of constant thickness d_{liq} on a surface and irradiated with a laser beam of cross sectional area A the detected induced fluorescence intensity at position (x,y), I_{LIF}, is proportional to

$$I_{LIF}(x,y) = Q_D \, \phi \, I_L(x,y) \, n_{tr} \, \sigma_{tr} \, d_{liq}, \qquad (1)$$

where ϕ is the fluorescence quantum yield and σ_{tr} the absorption cross section of the tracer. The factor Q_D takes into account transmission characteristics of used optics, detection solid angle and efficiency, etc., and can be determined through calibration, i.e., a measurement with a liquid film of known thickness with all other parameters (laser intensity, spatial arrangement, etc.) kept the same as during the later data collection.

The excitation laser simultaneously induces spontaneous Raman scattering (RS) from the liquid solvent (water in our case) with a corresponding signal intensity of

$$I_{RS}(x,y) = Q_D \, I_L(x,y) \, n_{H2O} \left(\frac{d\sigma}{d\Omega} \right)_{H2O} d_{liq}, \qquad (2)$$

* Corresponding author: thomas.dreier@uni-due.de

where $(d\sigma/d\Omega)_{H2O}$ is the differential scattering cross section of liquid water (1.8×10^{-28} cm²/(sr · molecule) at 266 nm [4]). Although the Raman scattering cross section is several orders of magnitude smaller than $\phi\,\sigma_{tr}$ in Equation (1) the large number density of the solvent still cases a sizable signal, with the additional benefit of being a tracer-free detection method.

Finally, for a NIR laser beam at a frequency ν_i crossing through the absorbing liquid film a transmission of

$$\tau_{DLAS}(x,y,\nu_i) = \frac{I_t(\nu_i)}{I_0(\nu_i)}(1-u)\exp(-n_{H2O}\sigma(\nu_i,T_l)\,d_{liq}) \qquad (3)$$

can be determined. In this equation $\sigma(\nu_i,T_l)$ is the absorption cross section of liquid water at frequency ν_i and temperature T_l., and u the fraction of "non-specific" absorption not related to liquid water, but possible impurities within the liquid and/or on the surface. This parameter, as well as temperature and thickness of the liquid can be determined individually by forming transmission signal ratios from at least four laser beams with appropriately positioned frequencies [5]. As a method of film thickness measurement without tracers in the present context DLAS is and independent tool for validating the LIF diagnostics with respect to preferential tracer evaporation [5].

Measurement strategies

For LIF and Raman imaging a UV laser beam of appropriate cross-section illuminates the liquid film spread out on a (in this case transparent) surface and the spatially extended signal from the liquid is monitored with an intensified CCD-camera. Provided other experimental parameters remain unchanged and the fluid is at constant temperature, the amount of signal collected on each pixel of the CCD detector is proportional to the illuminated and imaged probe volume. In the case of LIF an organic tracer (ethyl-acetoacetate, EAA) added at low concentration (0.1% by weight) serves as the fluorescent agent. Figure 1 shows the absorption cross section (solid squares with error bars, left panel) and the (peak normalized) fluorescence spectrum (right panel) of EAA when excited at the wavelength of the fourth harmonic of a Nd:YAG-laser (266 nm).

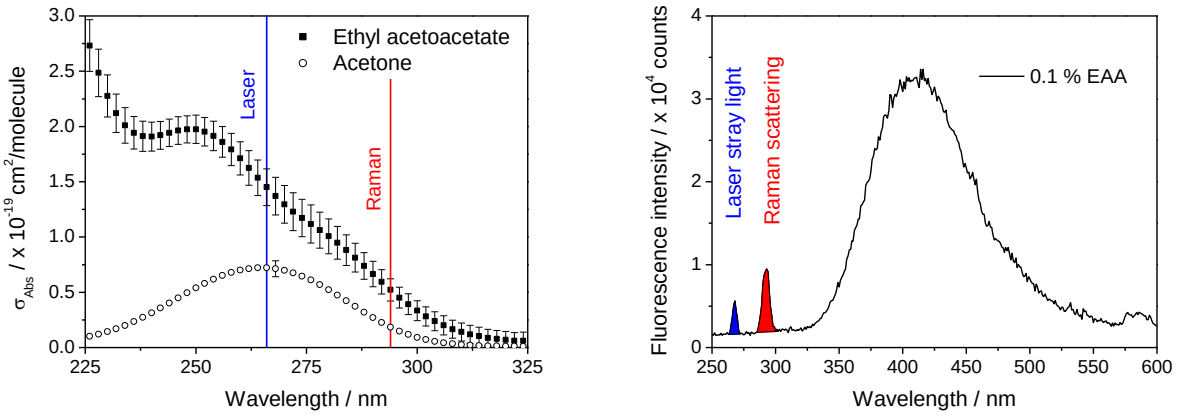

Figure 1 Left: Absorption cross section of EAA (solid squares) and acetone (open circles, from [6]) in the near UV spectral region. Also shown as vertical line markers are the wavelength positions of the excitation laser used in the present experiments and the center region of the Stokes-shifted Raman band of liquid water (also see right panel); Right: Fluorescence spectrum of EAA after excitation at 266 nm. The colored bands are the residual stray light and the Raman band of liquid water.

The comparison with acetone the absorption spectrum (open circles in Fig. 1, data from [6]) shows that EAA exhibits roughly a factor of two larger absorption cross-sections at the laser wavelength. For both diagnostic methods the generated signals are selected by appropriate filters and imaged on separate areas on the camera chip via an image doubler in front of the camera lens. Signal intensities must be calibrated in separate experiments with a water film of known thickness and possible attenuation of the laser beam and emerging signal photon flux when traversing the liquid must be taken into account [5]. Figure 2 shows the measured signal (mean value of pixel counts within a region of interest) as a function of film thickness, the latter being known from the separation of two quartz plates between which the liquid was enclosed in a custom-built calibration tool. The latter consists of a stainless steel trough fitted with one quartz plate into the bottom and

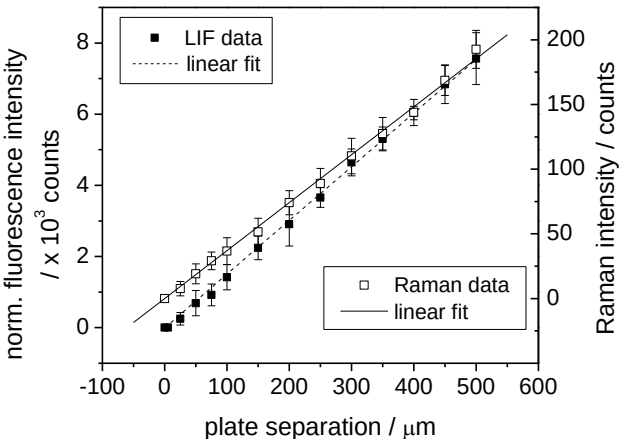

Figure 2 Dependence of measured LIF/Raman signal intensities on thickness of a water film of known thickness (see text for explanations).

filled with a water/EAA solution, while the second plate was fixed in a mirror mount attached on a translation stage for adjusting it to the desired plate separation [7].

Contrary to the LIF and Raman techniques absorption techniques do not require calibration once the absorption cross section is known. Additionally, for determining the temperature of liquid water the NIR-DLAS method exploits the fact that the absorption spectrum in the near infrared is temperature dependent (cf., Fig. 3, left panel) [8].

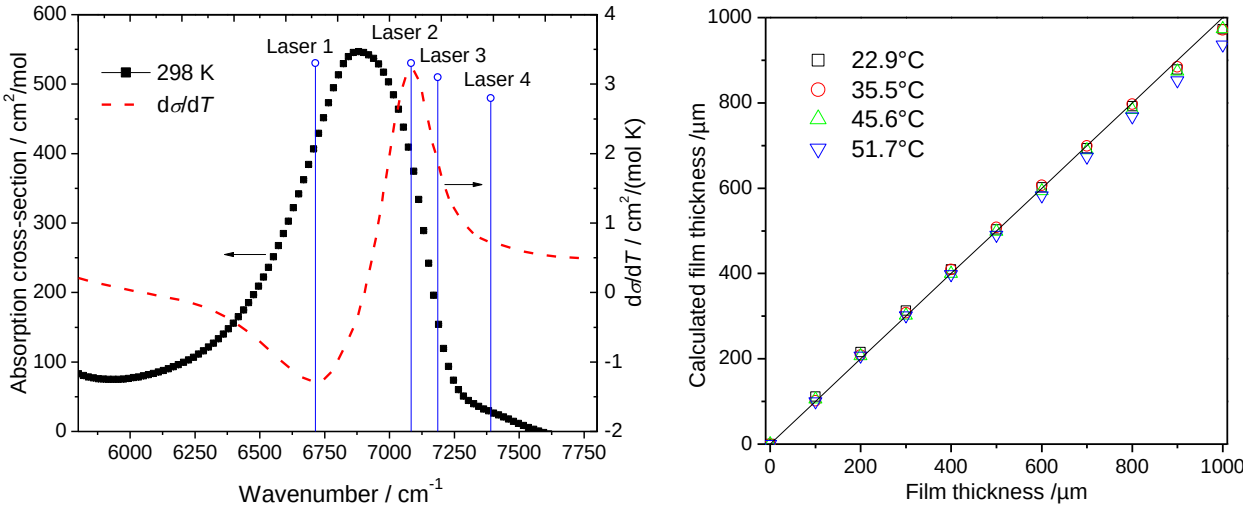

Figure 3 Left: Absorption spectrum of liquid water (solid squares) and its derivative with respect to temperature (dashed line), together with wavenumber positions of diode lasers used in the present experiment (circles with drop lines). Right: Liquid water film thickness calculated from absorption ratios vs. given plate separation at four temperatures.

Therefore, measuring the absorption at four appropriate NIR wavelengths (i.e., time multiplexing four diode laser beams transmitting the liquid layer) in the 6500–7500 cm^{-1} range (drop lines in Fig. 3) and forming appropriate transmission ratios [7] enables the simultaneous determination of temperature and film thickness. Specifically, from the ratio of the transmittance ratios at wavenumber positions (i,k), $\ln(R_{i,k}) = \sigma_k - \sigma_i$, using lasers (1,2) and (1,4), respectively, the temperature of the liquid is determined, which then allows evaluating the film thickness via the absorbance ratios $a_i = \ln(I_t/I_0)_i$ of lasers 1 and 2:

$$d_{liq} = \frac{a_1 / a_2}{n_{H2O}(\sigma_1 - \sigma_2)} \qquad (4)$$

A validation of this technique was performed using the calibration tool mentioned above (cf., Fig. 3, right panel).

Experimental setup

All measurements were performed in a horizontal air-fed flow tunnel with a square cross-section (50×50 mm^2) and a length of 1400 mm (Fig. 4). Optical access was provided by quartz windows in all sidewalls of the central channel, where in addition the upper wall supported a three-hole injection nozzle through which the liquid was injected towards the lower quartz window with injection durations of 300 ms. Air flow through the channel was provided by a radial blower and approached 7.5 m/s at the channel centerline. For the combined LIF/Raman imaging a frequency-quadrupled Nd:YAG-laser (Litron Lasers, Nano L PIV) beam at 266 nm was coupled into a guiding arm with its other end positioned above the channel, where it was directed through a diverging spherical lens and the top window through the liquid deposited onto the bottom window. At that position the beam energy was 6 mJ with and illuminated area of 45 mm in diameter. Shot-to-shot laser energy variation was monitored by detecting fluorescence from a dye cell illuminated by a split-off fraction of the beam and directed through an optical fiber and a small prism onto the camera sensor (see Fig. 4).

Raman scattered or fluorescence light from the sample passed an image doubler (LaVision) and was collected by a UV achromat (Coastal Optics, f = 105 mm, $f_\#$ = 4.0) attached to an ICCD camera (LaVision, StreakStar). The EAA-LIF signal (330–530 nm) was discriminated against laser stray light by a long pass filter (Schott, WG320) [9]. A neutral density filter attenuated the LIF signal to levels typical of the Raman detection channel. The Raman signal (Stokes shift: 3200–3600 cm^{-1}) was discriminated against EAA-LIF and laser stray light with a bandpass filter (Laser Components, 290 nm) and a long-pass edge filter (Semrock, RazorEdge 266RS), respectively. Signal intensities were calibrated for film thickness by placing a thin cell consisting of two quartz plates separated by a spacer of known thickness with the gap filled with the sample liquid onto the lower support window in the channel and taking images with known laser fluence. The linearity of the LIF/Raman signal with film thickness was previously checked using the procedure outlined above (see Fig. 9 [9]).

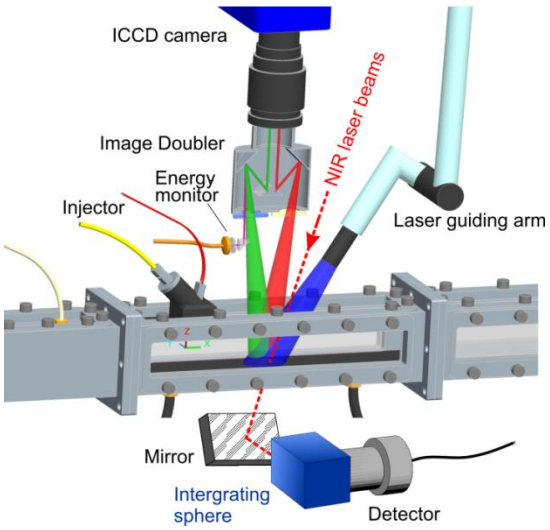

Figure 4 Optically accessible flow tunnel for the study of liquid water film thickness imaging using simultaneous LIF / Raman imaging. The point-wise measurement of film thickness and temperature of the liquid by NIR-DLAS from within the laser-illuminated film is also shown.

For the LIF measurements ethyl-acetoacetate (EAA) was chosen as tracers due to its high quantum yield and good water solubility. With respect to its co-evaporative behavior in the temperature range of interest, as was deduced from vapor-liquid equilibrium calculations, it performs better than, e.g., acetone or 3-pentanone commonly used with hydrocarbon solvents.

The NIR-DLAS setup for point-wise liquid water film temperature and thickness measurement – simultaneously with either the LIF or Raman imaging technique – is also shown in Fig. 4. The four diode lasers were time multiplexed with each laser switched on for 3 ms, and the transmitted beams were captured by an integrating sphere (Thorlabs) to reduce the effect of beam steering when passed though media with temporally and spatially varying shape and surface ripple. Signals were recorded by a single InGaAs photodiode (Thorlabs, PDA10CS-EC) before feeding a data acquisition system (National Instruments).

Results and discussion

Figure 5 shows typical 25-shot average thickness images evaluated from the Raman (left) and LIF (right) images taken after injection. The water films deposited from the three-hole injector on the bottom wall are clearly identified, with a thickness profile along the white horizontal line through the right droplet depicted below each image.

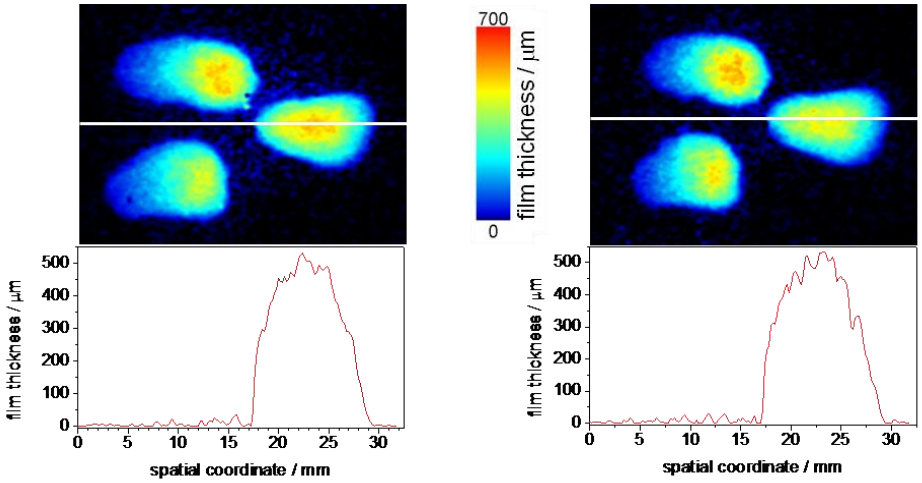

Figure 5 25-shot average of planar thickness images (upper row) evaluated from the corresponding LIF (left) and Raman (right) images. Lower row: corresponding film thickness profiles along the white lines. Spray injection and tunnel flow were from left to right in the images.

Taking images after varying time delays between activating the nozzle and laser firing allowed phase resolved droplet imaging during the impingement process of the spray onto the lower flow channel wall. Figure 6 shows 50-shot averaged images of film thickness taken at the given temporal delays after start of injection (aSOI).

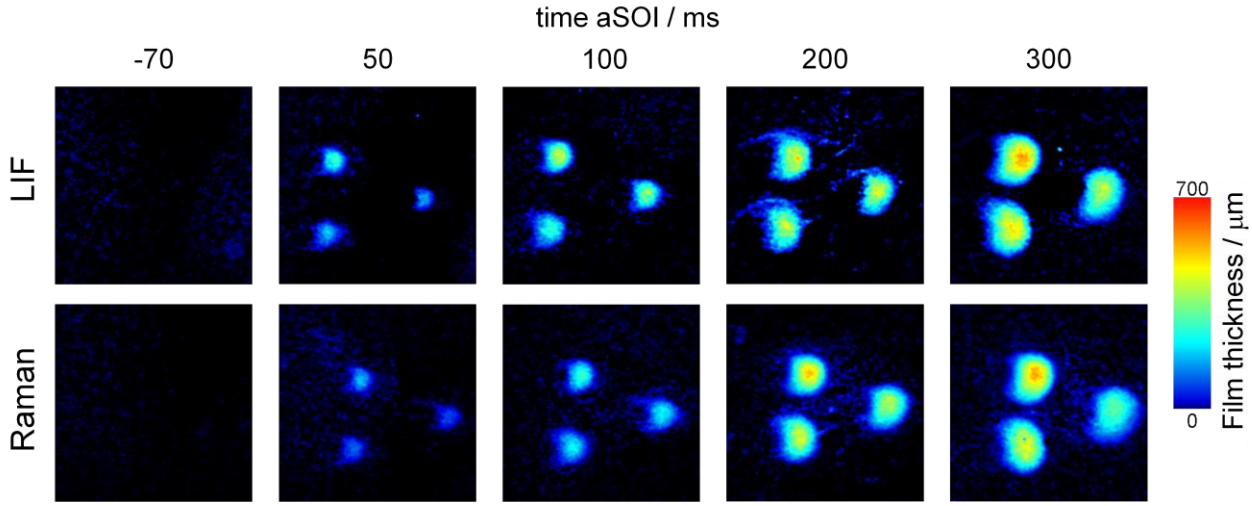

Figure 6 50-shot average of water thickness evaluated from the LIF (upper row) and Raman (lower row) detection channels for a spray impinging on the lower flow channel wall. The temporal delay between activation of the injector and laser firing is indicated.

It is observed that the tips of the spray cones are visible in the images with acceptable signal levels after approximately 50 ms. This time corresponds to the instant the spray cones hit the support window and thus are in the focal plane of the camera lens. At later times the contract area of each spray cone increases and approximately stays constant when all ejected liquid has deposited on the window (injection duration: 100 ms). As is observed in the LIF images at 200 ms aSOI, waves are formed near the rim of each impingement area during the droplet splash which then decay after the end of injection.

To study dynamic film behavior the three thickness diagnostics methods were applied to a liquid film evaporation process taking place during active air flow in the flow duct of Fig. 4. Figure 7 shows the variation of water layer thickness with time of one of the water patches from Fig. 5 after injection for both the LIF (open symbols) and Raman (filled symbols) image detection channels without (left) and with (right) air flow through the tunnel. During the measurement the window supporting the liquid was heated by a hot air flow from outside to approx. 55°C to speed up the evaporation process. From the recorded images the counts of a 3×3 pixel area from the center region of the right most droplet patch in Fig. 5 were summed and plotted vs. time. In both cases, during the initial phase of the evaporation process the Raman and LIF data follow the same trend with time, while towards the end (at small film thickness) the thickness values deduced from the LIF data tend to be smaller with respect to the Raman data, where the latter may serve as a validation for the ability of the tracer to co-evaporate with the solvent [6].

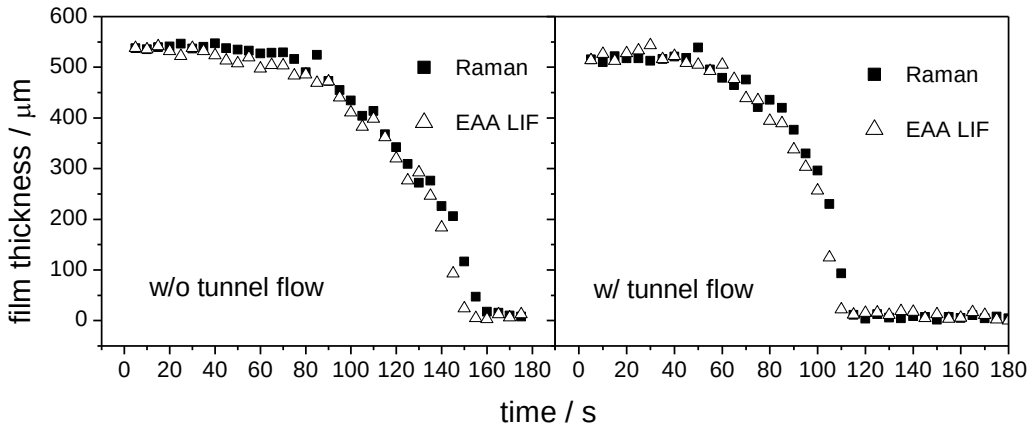

Figure 7 Temporal development of liquid water film thickness after spray deposition without (left) and with (right) air tunnel flow; evaluation is from the Raman and LIF detection channels, respectively.

A similar experiment was conducted using the DLAS setup described above by pointing the multiplexed NIR laser beams through the center region of the selected film area into the integrating sphere as shown in Fig. 4. In Fig. 8 is plotted the temporal development of the measured film thickness as a function of time after actuating the injector, without (left panel) and with (right panel) tunnel air flow.

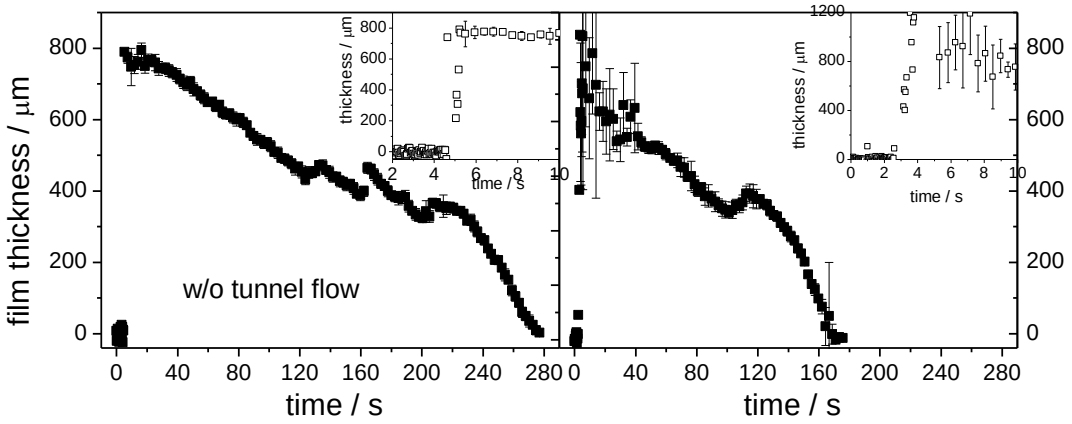

Figure 8 Film thickness variation of an impinging water jet, with subsequent film evaporation as a function of time in the flow tunnel without (left) and with (right) active air flow. Insets: Film thickness variation within the first 10 s.

As in the previous case the temporal thickness development of one of the three droplets deposited onto the lower channel wall was studied. The graphs depict the injection-evaporation process for from before the spray cone hits the support window (thickness values below the detection limit) until most liquid is evaporated within the beam cross section. In the case without air flow (left panel), during impingement of the water jet hitting the laser beam interaction region the film thickness suddenly increased from zero to ~ 800 µm during a time span of 0.5 s after the beginning of data acquisition (BODA). Subsequently, the evaporation process leads to an almost linear decrease of the film thickness interrupted by several sudden steps (in this case at 130, 160, and 210 s after BODA, respectively), possibly due to a recombination or rearrangement of the three deposited water droplets on the plate. For the case with an active air flow (right panel) the retrieved thickness variation shows a much stronger fluctuation with a standard deviation of more than ±100 µm within the first 60 s after BODA. This observation have been caused by small air bubbles formed in the liquid and their vibration in the air flow leading to additional beam deflections/deformations not compensated completely by the signal ratio procedure and/or the integrating sphere in front of the detector. The whole evaporation process ceases approx. 180 s after BODA, roughly 35% earlier than without air flow.

Conclusions

Raman scattering, tracer LIF and NIR diode laser absorption were applied for the thickness measurement of liquid water films deposited on a glass wall and during evaporation in a strong tunnel air stream. Raman and LIF diagnostics enables imaging of film thickness and both techniques were applied simultaneously using a CCD camera. The Raman scattering and the absorption technique are tracer free, while for LIF imaging a molecular tracer with a large fluorescence quantum yield was added. For the LIF/Raman techniques measurements in real time depend on the repetition rate of the UV-laser and camera detector equipment used, whereas the data acquisition rate of the absorption method is dependent on the bandwidth of the time multiplexing and A/D-converter electronics (typically 1–100 kHz). The experimental arrangement shows potential to operate all three techniques simultaneously.

Acknowledgements

The financial support by the German Research Foundation (DFG) within the framework of GRK1114 and SFB445 is gratefully acknowledged.

References

[1] Cho, H., and Min, K., *Measurement of liquid fuel film distribution on the cylinder liner of a spark ignition engine using the laser-induced fluorescence technique*, Meas. Sci. Technol., 14: 975-982 (2003).

[2] Birkhold, F., Meingast, U., Wassermann, P., and Deutschmann, O., *Analysis of the injection of urea-water-solution for automotive SCR DeNOx-systems: modeling of two-phase flow and spray/wall-Interaction*, SAE Technical Paper Series, 2006-01-0643 (2006).

[3] Schulz, C., and Sick, V., *Tracer-LIF diagnostics: Quantitative measurement of fuel concentration, temperature and air/fuel ratio in practical combustion situations*, Progr. Energy Combust. Sci., 31: 75-121 (2005).

[4] Gregory, W. F., and Copeland, R. A., Appl. Opt., 36: 2686-2688 (1997).

[5] Greszik, D., Yang, H., Dreier, T., and Schulz, C., *Laser-based diagnostics for the measurement of liquid water film thickness.* Appl. Opt.,. 50: A60-67 (2011).

[6] Xu, H., Wentworth, P. J., Howell, N. W., and Joens, J. A., Spectrochimica Acta, 49A: 1171-1178 (1993).

[7] Yang, H., Greszik, D., Dreier, T., and Schulz, C., *Simultaneous measurement of liquid water film thickness and vapor temperature using near-infrared tunable diode laser spectroscopy.* Appl. Phys. B, 99: 385-390 (2010).

[8] Yang, H., Greszik, D., Wlokas, I., Dreier, T., and Schulz, C., *Tunable diode laser absorption sensor for the simultaneous measurement of water film thickness, liquid- and vapor-phase temperature*. Appl. Phys. B, 104: 21-27 (2011).

[9] Greszik, D., Yang, H., Dreier, T., and Schulz, C., *Measurement of water film thickness by laser-induced fluorescence and Raman imaging.* Appl. Phys. B, 102: 123-132 (2011).